Probing the reactivity of microhydrated α-nucleophile in the anionic gas-phase SN2 reaction

ARTICLE *in* JOURNAL OF COMPUTATIONAL CHEMISTRY · MARCH 2015

Impact Factor: 3.59 · DOI: 10.1002/jcc.23862 · Source: PubMed

15 AUTHORS, INCLUDING:

Jun Zhu

Xiamen University

65 PUBLICATIONS **887** CITATIONS

SEE PROFILE

Yi Ren

Sichuan University

67 PUBLICATIONS **776** CITATIONS

SEE PROFILE

THE JOURNAL OF PHYSICAL CHEMISTRY A

Article

pubs.acs.org/JPCA

Origin of Enhanced Reactivity of a Microsolvated Nucleophile in Ion Pair S_N2 Reactions: The Cases of Sodium *p*-Nitrophenoxide with Halomethanes in Acetone

Qiang-Gen Li,[†] Ke Xu,[‡] and Yi Ren*[,§]

[†]College of Chemistry and Material Science, Sichuan Normal University, Chengdu, 610068, People's Republic of China

[‡]School of Chemistry and Pharmaceutical Engineering, Sichuan University of Science and Engineering, Zigong, 643000, People's Republic of China

[§]College of Chemistry and Key State Laboratory of Biotherapy, Sichuan University, Chengdu 610064, People's Republic of China

Supporting Information

ABSTRACT: In a kinetic experiment on the S_N2 reaction of sodium *p*-nitrophenoxide with iodomethane in acetone−water mixed solvent, Humeres et al. (J. Org. Chem. 2001, 66, 1163) found that the reaction depends strongly on the medium, and the fastest rate constant was observed in pure acetone. The present work tries to explore why acetone can enhance the reactivity of the title reactions. Accordingly, we make a mechanistic study on the reactions of sodium *p*-nitrophenoxide with halomethanes (CH_3X, X = Cl, Br, I) in acetone by using a supramolecular/continuum model at the PCM-MP2/6-311+G(d,p)//B3LYP/6-311+G(d,p) level, in which the ion pair nucleophile is microsolvated by one to three acetone molecules. We compared the reactivity of the microsolvated ion pair nucleophiles with solvent-free ion pair and anionic ones. Our results clearly reveal that the microsolvated ion pair nucleophile is favorable for the S_N2 reactions; meanwhile, the origin of the enhanced reactivity induced by microsolvation of the nucleophile is discussed in terms of the geometries of transition state (TS) structures and activation strain model, suggesting that lower deformation energies and stronger interaction energies between the deformed reactants in the TS lead to the lower overall reaction barriers for the S_N2 reaction of microsolvated sodium *p*-nitrophenoxide toward halomethanes in acetone.

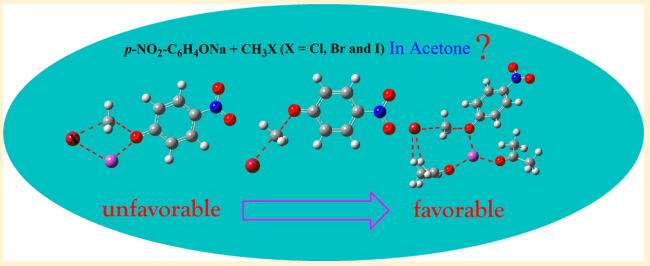

1. INTRODUCTION

The bimolecular nucleophilic substitution (S_N2) reaction is very significant to both chemical[1,2] and biochemical processes.[3] In the past decades, most attention has been focused on the anionic S_N2 reactions and relatively less on the ion pair ones.[4,5] In general, anions are considered as reactive species for S_N2 reactions in the gas phase, and their reactivity will significantly decrease in polar solvents.[5−11] The usual explanation is that the transition state with more charge dispersion is less solvated than the separated reactants, especially free anions, and results in a much higher activation barrier for the anionic S_N2 reaction in polar solvent than that in the gas phase. However, when reactions take place in nonpolar or less polar solvent, ion pairs will be formation by interacting with the counterion. In this case, the dominant nucleophilic species will be ion pairs instead of free ions.[11] Actually, many important organic reactions as well as biological processes usually involve neutral ion pairs as nucleophiles.[12−24] In recent years, the ion pair reaction has received increasing attention since its application has been discovered in the field of phase-transfer catalysis.[25]

In determining the rate constants of the S_N2 reaction of sodium *p*-nitrophenoxide and iodomethane by UV−visible spectrophotometry in acetone−water mixed solvent, it is found that the reaction depends strongly on the medium, and the fastest rate constant was obtained in pure acetone.[24] Considering that lithium bromide dissociates only slightly in pure acetone, we can also expect that sodium *p*-nitrophenoxide, instead of free *p*-nitrophenoxide anion, acts as a nucleophile in pure acetone; i.e., the ion pair S_N2 reaction is actually carried out.

It is well know that the reactivity of an ion pair nucleophile is rather different from that of an anionic one,[18,21−24] and theoretical investigations of ion pair S_N2 reactions are relatively scarce.[11−15,26−40] Two different reaction pathways were proposed for the ion pair S_N2 reactions in the gas phase, i.e., backside attack with inversion and frontside attack with retention of configuration. Both pathways are preceded via cyclic, highly strained transition states (TSs), leading to a higher reaction barrier than for the corresponding anionic reaction in the gas phase.[28,29,31,36,37] This result can be explained by the much weaker basicity of the neutral ion pair than of the free anionic nucleophile induced from partially

Received: February 1, 2015
Revised: April 1, 2015
Published: April 2, 2015

DOI: 10.1021/acs.jpca.5b01045
J. Phys. Chem. A 2015, 119, 3878−3886

neutralized nucleophile by counterion. Moreover, the ion pair S_N2 reaction involves the bond breaking of the ion pair, which will also consume energy and raise the barrier. There is a substantial correlation between the bond dissociation energy and the rate constant for ion pair S_N2 reactions.[16] Thus, ion pair S_N2 reaction has been considered to be unfavorable compared to the anionic S_N2 reaction in the gas phase.[28,29,37]

In solution phase, ion pair S_N2 reactions are still affected by both the intrinsic reactivity and the solvent effect, but a neutral ion pair is expected to be less sensitive to solvation. In fact, in less polar protic or polar aprotic solvents, the existence of the countercation and solvent surroundings can accelerate the reaction greatly. This has been confirmed by recent experimental and theoretical studies of the ion pair S_N2 reaction.[11,13−15,19,24] These studies found the promoting role of explicit solvent molecules by coordinating cations and also compared the relative reactivity of free ions and ion pairs in S_N2 reactions.[11,13−16,40] However, no systematic theoretical analysis is available regarding the origin of the enhanced reactivity for the S_N2 reaction in polar aprotic solvent.

The polarized continuum model (PCM)[41] based on the self-consistent reaction field (SCRF) is a very powerful and popular method in the presence of a solvent, and it allows a quantum mechanical description of the solute in a solvent continuum at a lower computational cost. However, this model was inadequate to describe the real reaction system in some cases where there are some important and specific solute−solvent electrostatic interactions. An alternative and effective approach may be the combined supramolecular/continuum model,[11,13−16,26,27] in which the nucleophile is microsolvated by a number of explicit solvent molecules. The microsolvated reaction system is optimized by quantum chemical methods, and the bulk solvation effect is incorporated by application of the PCM method. In this way, both of the short- and long-range interactions are considered.

To explore the mechanism of the title reaction in pure acetone, the present study will make a comprehensive theoretical study on the reactivity of an ion pair nucleophile in acetone solution. For the comparison of the kinetic performance of different nucleophiles, three possible reactants will be served as nucleophiles toward CH_3X, (X = Cl, Br, and I), respectively, i.e., *p*-nitrophenoxide anion, sodium *p*-nitrophenoxide, and microsolvated sodium *p*-nitrophenoxide (eqs 1−3).

$$p\text{-}NO_2{-}C_6H_4O^- + CH_3X = p\text{-}NO_2{-}C_6H_4OCH_3 + X^- \quad (1)$$

$$p\text{-}NO_2{-}C_6H_4ONa + CH_3X = p\text{-}NO_2{-}C_6H_4OCH_3 + NaX \quad (2)$$

$$p\text{-}NO_2{-}C_6H_4ONa{\cdot}n\text{Ace}\ (n = 1{-}3) + CH_3X = p\text{-}NO_2{-}C_6H_4OCH_3 + NaX{\cdot}n\text{Ace}\ (n = 1{-}3) \quad (3)$$

X = Cl, Br, and I; Ace = acetone

There are a few objectives for the present paper: (1) to compare the TS geometries and the reactivity of free anion, solvent-free ion pair nucleophile, and microsolvated ion pair nucleophile; (2) to evaluate how many explicit solvent molecules binding to ion pair nucleophile is favorable for the title reactions; (3) to probe why pure acetone can increase the rate of the title reactions by using the activation strain model. We think the present study is helpful for better understanding of the S_N2 reaction in polar aprotic solvent.

2. COMPUTATIONAL DETAILS

All species involved in the reactions (eqs 1−3) were fully optimized without symmetry constraints with the B3LYP[42−44] method in combination with 6-311+G(d,p) basis sets. This DFT approach has been selected because it has been successfully applied in previous studies on the S_N2 reaction,[45−51] as well as in our recent investigation on the effects of substituent and leaving group.[52] The optimized structures were characterized as minima (no imaginary frequency) or transition state (only one imaginary frequency) by the vibrational frequency analysis at the same level. Unscaled frequencies are applied to the zero-point vibration energy (ZPVE) corrections, and thermal and entropy corrections computed by standard statistical methods were used in the calculations of relative energies. The energies were further refined by additional single-point calculations at the MP2/6-311+G(d,p) level.

The bulk solvent effect on reactivity is calculated with the applied PCM approach,[41] which was used in the previous studies on the ion pair S_N2 reactions.[14,26,39,40] Accordingly, the energies of species in acetone (ε = 20.493) are obtained by a single-point PCM calculation at the MP2/6-311+G(d,p) level based on the DFT-optimized geometries, denoted as PCM-MP2 6-311+G(d,p)//B3LYP/6-311+G(d,p).

The effective core potentials (ECP) of Wadt and Hay[53] were used for bromine and iodine atoms in the B3LYP optimizations in the gas phase and MP2 single-point calculations in the gas phase and in solution.

Throughout this study, all calculations were performed using the Gaussian 09 program.[54] All internuclear distances are in angstroms and all angles are in degrees. The relative energy (kJ/mol) is described by electronic energy change without ZPVE correction, ΔE, which is from MP2//6-311+G(d,p) single-point calculation in the gas phase or in acetone solution (denoted as PCM-ΔE), and the Gibbs free energy change, ΔG, is determined by adding the B3LYP/6-311+G(d,p) free energy correction to the single-point energy at MP2/6-311+G(d,p) in the gas phase or in acetone solution (denoted as PCM-ΔG).

In order to show the rationality of the present methodology, we have optimized the S_N2 reaction of $p\text{-}NO_2{-}C_6H_4O^-$ anion toward CH_3Cl in acetone by PCM-B3LYP and compared the PCM-MP2/6-311+G(d,p)//PCM-B3LYP/6-311+G(d,p) result with the one from PCM-MP2 6-311+G(d,p)//B3LYP/6-311+ G(d,p). It is found that the overall barrier, ΔG^b, is 132.2 kJ/mol by the PCM-B3LYP optimization in acetone, only slightly higher than the B3LYP optimization result in the gas phase by 4.2 kJ/mol.

3. RESULTS AND DISCUSSION

The energy profile of S_N2 reactions toward halomethanes (CH_3X, X = Cl, Br, and I) is described by an asymmetrical double-well curve (see Scheme 1). Initially, the reactants (Re) form a loosely bound reactant complex (RC). This RC must then overcome the central barrier ($\Delta E^{\ddagger}$) to reach an asymmetrical transition state (TS). The latter then breaks down to give the product complex (PC), accompanying the formation of the C−O bond and cleavage of the C−X bond. Subsequently, the PC dissociates into the separate products (Pr).

DOI: 10.1021/acs.jpca.5b01045
J. Phys. Chem. A 2015, 119, 3878−3886

Scheme 1. Schematic Potential Energy Profile for the Title Reactions

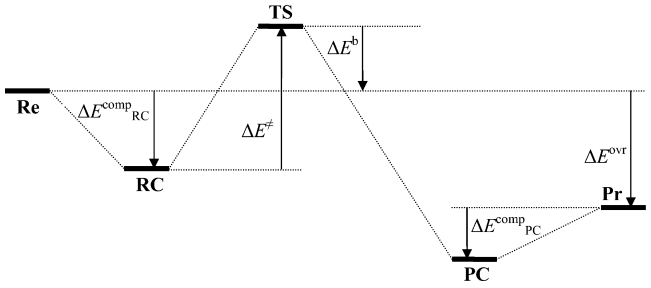

3.1. Anionic and Solvent-Free Ion Pair S_N2 Reactions.

First of all, we check the anionic and ion pair S_N2 reactions of *p*-nitrophenoxide anion and sodium *p*-nitrophenoxide toward CH_3X (X= Cl, Br, and I). It is well-known that the inversion pathway in an anionic S_N2 reaction is much more favorable than the retention one.[55−57] However, the two reaction mechanisms are competitive sometimes in the ion pair S_N2 reaction.[28,31,34] Therefore, only the inversion pathway is considered for the anionic reaction, whereas both pathways are calculated for the solvent-free ion pair reaction in present study.

The geometrical parameters for CH_3X and NaX (X = Cl, Br and I) are listed in Table S1 (see Supporting Information). The relative energies of all species involved in the anionic and solvent-free ion pair reactions are summarized in Tables 1 and 2, and the important geometries for both kinds of reactions are presented in Figures 1−3.

3.1.1. Reactants, Products, and Reactants Complex. The B3LYP-optimized C−X and C−H in CH_3X and Na−X bond lengths in NaX are in agreement with the CCSD(T) results[58] and experiments.[59−63] Compared with the experimental data, the largest deviations for the C−X (0.035 Å) and C−H bond lengths (0.004 Å) in CH_3X and Na−X bond lengths (0.038 Å) in NaX are found for X = Br. Furthermore, the X−C−H angles deviate from the experiments only by up to 1.0° (X = I), indicating that the present computational method is reliable in the optimization.

For the anionic S_N2 reactions, the O2···H3 bond length in ion−molecule RC is sensitive to variations of substrate and decreases with the reduction of the electronegativity of X in substrate (see Figure 2). The O2···H3 bond is shorter than the corresponding O2···H6 bond in solvent-free ion pair dipole−dipole RC by 0.085 Å (X = Cl), 0.139 Å (X = Br), and 0.193 Å (X = I), respectively, but there is another electrostatic interaction between sodium and halogen atom with the Na−X distance of 2.732−3.098 Å, leading to the lower complexation electronic energies (PCM-ΔE^{comp}_{RC}) of dipole−dipole RC than ion−molecule RC by 7.5 kJ/mol (X = Cl), 15.9 kJ/mol (X = Br), and 14.2 kJ/mol (X = I). Due to the entropy effect, the complexation Gibbs free energies (PCM-ΔG^{comp}_{RC}) become positive for both anionic and solvent-free ion pair S_N2 reactions, suggesting that these complexes are unstable in acetone solution.

3.1.2. TS Structures and Barrier Heights. As shown in Figure 2, the anionic S_N2 inversion TSs present linear conformations, in which the angle of the O2···C5···X4 moiety is close to 180°, and the C5−O2 bond lengths increase in the order X = Cl < Br < I. It may be attributed to the increment of the leaving ability I > Br > Cl; thus, an earlier TS structure feature is found for the better leaving group, accompanying the increase of C−X bond order from Cl to Br to I. The TS structure with the less negatively charged and good leaving group will reduce the solvation energy in polar solvent. This is further proved by the PCM-MP2 calculations (see Table 2), where the overall barriers in acetone (PCM-ΔG^{b}) are 128.0 kJ/mol (X = Cl), 98.7 kJ/mol (X = Br) and 98.7 kJ/mol (X = I) for the anionic reactions, which is slightly different from the intrinsic leaving ability in the gas phase.

For the solvent-free ion pair S_N2 reactions, as mentioned above, both inversion and retention pathways are considered. The geometries in the inversion and retention TSs (see Figure 3) show that they are significantly deformed from the linear structures. The bridging of Na^+ causes a large decrease of O2−C5−X4 angles by 49.7°−52.0° for the inversion TS and 92.6°−95.2° for the retention TS. The decrease of the angle O2−C5−X4 will increase the electrostatic repulsion between $O2^-\cdots X4^-$ and thus destabilize the ion pair TS relative to the anionic TS.

Table 1. Reactants and Products Complexation Electronic Energies (ΔE^{comp}_{RC}, ΔE^{comp}_{PC}), Central Barriers ($\Delta E^{\ddagger}$), Overall Barriers (ΔE^{b}), and Overall Reaction Energies (ΔE^{ovr}) for All Species in the Title Reactions[a]

X	Nu	ΔE^{comp}_{RC}	$\Delta E^{\ddagger}$	ΔE^{b}	ΔE^{comp}_{PC}	ΔE^{ovr}
Cl	Nu^-	−4.6	85.8	81.2	−0.8	−77.8
	0Ace···Nu	−12.1	198.3 (216.7)[b]	186.2 (228.9)	0.8	−69.0
	1Ace···Nu	−16.7	91.6	74.9	−2.1	−70.7
	2Ace···Nu	−23.4	90.0	66.5	−7.5	−65.7
	3Ace···Nu	−25.9	89.1	63.2	−33.9	−53.6
Br	Nu^-	−13.4	64.9	51.5	−15.5	−104.6
	0Ace···Nu	−29.3	192.0 (219.7)	162.8 (190.4)	−18.8	−84.9
	1Ace···Nu	−13.4	66.9	53.6	−9.2	−87.0
	2Ace···Nu	−22.6	69.5	46.4	−13.8	−84.5
	3Ace···Nu	−23.0	69.0	46.0	−33.5	−74.5
I	Nu^-	−14.2	66.1	51.9	−18.4	−108.4
	0Ace···Nu	−28.5	154.8 (164.0)	126.4 (192.5)	−15.1	−84.9
	1Ace···Nu	−13.4	45.2	31.8	−10.9	−88.7
	2Ace···Nu	−22.6	63.2	40.6	−11.7	−87.9
	3Ace···Nu	−23.0	66.9	44.4	−36.0	−79.1

[a]All of relative energies are from PCM-MP2/6-311+G(d,p) single-point calculations in acetone on B3LYP gas-phase geometries without ZPVE corrections (in kJ/mol). [b]Values in parentheses are corresponding energies of retention pathways.

DOI: 10.1021/acs.jpca.5b01045
J. Phys. Chem. A 2015, 119, 3878−3886

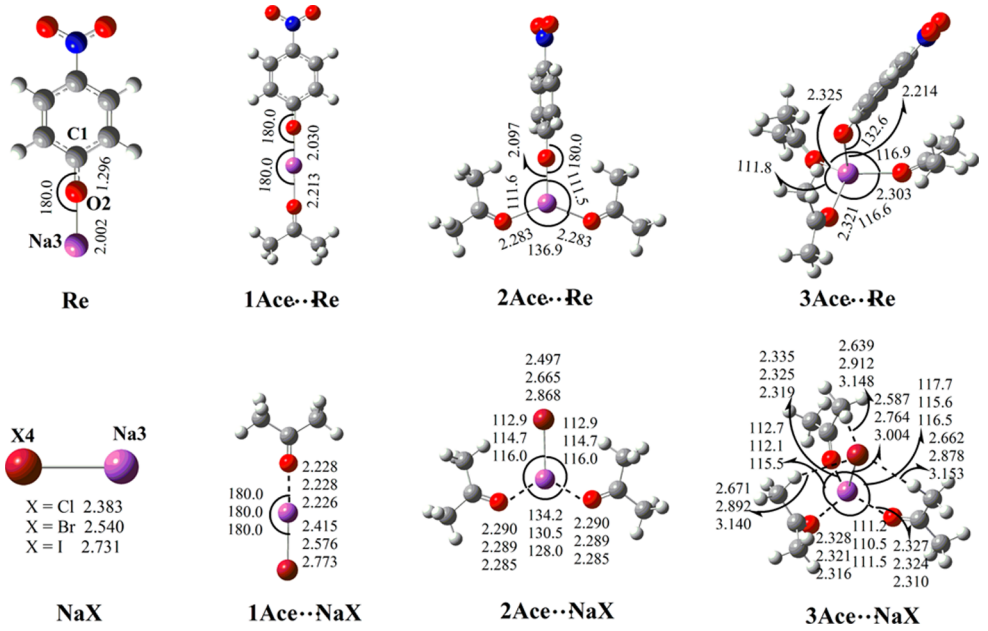

Figure 1. B3LYP/6-311+G(d,p)-optimized reactants complex *n*Ace···Re and products complex *n*Ace···NaX (*n* = 0−3; Re = *p*-NO_2−C_6H_4ONa), where X = Cl (top numbers), Br (center numbers), and I (bottom numbers).

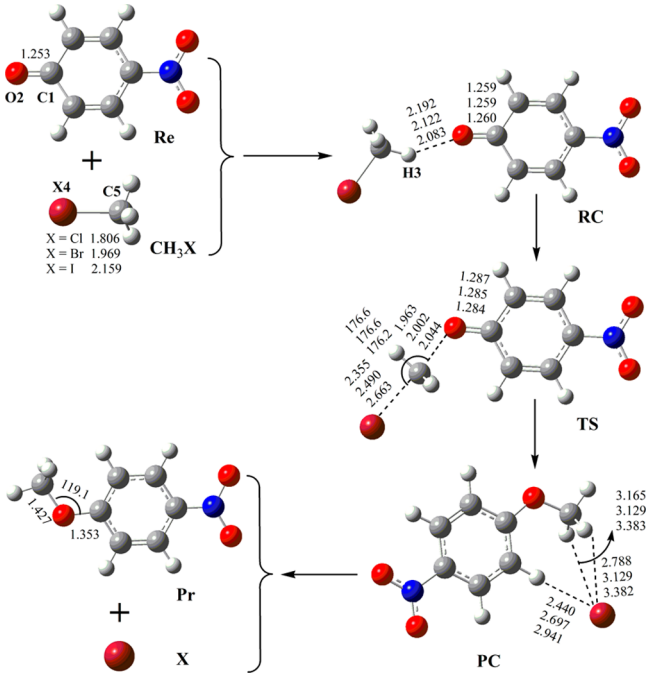

Figure 2. B3LYP/6-311+G(d,p)-optimized structures in the anionic S_N2 reactions *p*-NO_2−$C_6H_4O^-$ + CH_3X = *p*-NO_2−$C_6H_4OCH_3$ + X^- (X = Cl, Br, and I).

Furthermore, the C5−O2 and C5−X4 bond distances in the ion pair TSs are 2.076, 2.456 Å (X = Cl), 2.077, 2.612 Å (X = Br), and 2.079, 2.810 Å (X = I) for the inversion pathway and 2.284, 2.759 Å (X = Cl), 2.293, 2.947 Å (X = Br), and 2.304, 3.189 Å (X = I) for the retention pathway, respectively, longer than the corresponding values in the anionic TS. The significant deformation of TS structures will result in much higher reaction barriers for the solvent-free ion pair reactions than the anionic S_N2 reactions. The results in Table 2 show that the PCM-ΔG^b values of ion pair S_N2 reaction are 230.1 and 267.4 kJ/mol (X = Cl), 205.4 and 230.1 kJ/mol (X = Br), and 171.5 and 233.0 kJ/mol (X = I) for the inversion and retention pathway, respectively, higher than the inversion barriers in the anionic reaction by more than 71.1 and 133.9 kJ/mol, respectively. These results indicate that the inversion mechanism is more favorable for the ion pair S_N2 reactions; meanwhile, the solvent-free ion pair is not an active nucleophile in acetone due to the much higher barrier height of the ion pair TS.

3.2. Microsolvated Ion Pair S_N2 Reaction. It was experimentally found that for the S_N2 reaction of sodium *p*-nitrophenoxide with iodomethane, the specific solute−solvent interactions exist in the acetone-rich region, and the rate constant in pure acetone is faster than that of the anionic reaction in water.[24] Herein, we will apply the microsolvation model to explore how many explicit solvent molecules are involved in the title reaction and the role of solvent molecules by comparing the geometries and relative energies between microsolvated and solvent-free ion pair S_N2 reactions.

The previous studies[12,64] disclosed that one to four solvent molecules can coordinate on the alkali metal. Therefore, herein we introduce a microsolvation model constructed by one to three explicit acetone molecules and sodium *p*-nitrophenoxide to study the S_N2 reaction in pure acetone, in which the sodium atom is coordinated by one to three oxygen atom(s) on acetone (see Figure 2). Only the inversion pathway is discussed in the following on the basis of the above comparison between two pathways for the solvent-free ion pair S_N2 reaction. The geometrical structures for ion pair S_N2 reactions involving the mono-, di-, and trisolvated nucleophiles are displayed in Figures 1 and 4. The relative energies in acetone are summarized in Tables 1 and 2.

3.2.1. Microsolvated Reactants Complex. In the ion pair S_N2 reactions with microsolvated nucleophile, there are two stronger interactions between microsolvated sodium *p*-nitrophenoxide and CH_3X in the reactant complex (*n*Ace···RC). One interaction is from the positively charged sodium and negatively charged X atom in CH_3X, and other is from the phenyl oxygen and hydrogen atom on CH_3X, which is similar

DOI: 10.1021/acs.jpca.5b01045
J. Phys. Chem. A 2015, 119, 3878−3886

Table 2. PCM-MP2/6-311+G(d,p)//B3LYP6-311+G(d,p) Reactants and Products Complexation Gibbs Free Energies (ΔG^{comp}_{RC}, ΔG^{comp}_{PC}), Central Free Energy of Activation ($\Delta G^{‡}$), Overall Free Energy of Activation (ΔG^{b}), and Overall Reaction Free Energies (ΔG^{ovr}, kJ/mol) for All Species in the Title Reactions in Acetone

X	Nu	ΔG^{comp}_{RC}	$\Delta G^{‡}$	ΔG^{b}	ΔG^{comp}_{PC}	ΔG^{ovr}
Cl	Nu^-	21.8	106.3	128.0	24.7	−51.9
	0Ace···Nu	28.5	201.7 (238.9)[a]	230.1 (267.4)	40.2	−54.4
	1Ace···Nu	23.8	110.9	134.7	48.5	−58.2
	2Ace···Nu	11.3	105.0	116.3	40.2	−56.9
	3Ace···Nu	10.9	98.7	109.6	24.3	−50.2
Br	Nu^-	18.0	80.8	98.7	8.4	−77.0
	0Ace···Nu	10.0	195.4 (220.1)	205.4 (230.1)	11.3	−69.0
	1Ace···Nu	25.9	87.4	113.4	42.3	−76.6
	2Ace···Nu	11.7	85.8	97.5	32.6	−74.1
	3Ace···Nu	19.7	73.2	92.9	14.6	−64.9
I	Nu^-	17.2	81.6	98.7	7.1	−79.1
	0Ace···Nu	11.3	160.2 (221.8)	171.5 (233.0)	23.4	−68.2
	1Ace···Nu	26.8	65.3	92.0	42.3	−77.4
	2Ace···Nu	12.1	79.9	92.0	34.3	−77.4
	3Ace···Nu	23.4	71.5	95.0	13.0	−64.9

[a]Values in parentheses are corresponding energies of retention pathways.

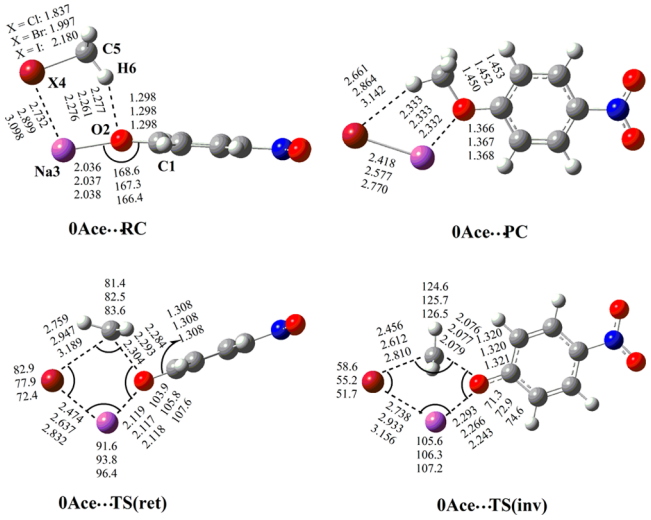

Figure 3. B3LYP/6-311+G(d,p)-optimized structures in the solvent-free ion pair S_N2 reactions *p*-NO_2−C_6H_4ONa + CH_3X = *p*-NO_2−$C_6H_4OCH_3$ + NaX (X = Cl, Br and I).

to the ion pair RC. For the di- and trisolvation models, the interactions exist between active hydrogen atoms on acetone and X atom, instead of direct Na···X interaction. These interactions will moderately change the structures of the microsolvated RC relative to solvent-free ion pair RC (see Figures 3 and 4). The C1−O2 bond length in *n*Ace···RC decreases from about 1.298 Å (solvent-free, $n = 0$) to 1.293 Å ($n = 1$), to 1.287 Å ($n = 2$), and to 1.286 Å ($n = 3$). Meanwhile, the Na−O bond length increases from 2.037 Å ($n = 0$) to 2.202 Å ($n = 3$), revealing that the C1−O2 bond has a double bond character, and the Na−O bond is almost broken with the successive coordination of acetone molecules on the sodium atom. Furthermore, the O2···H6 and the C5−X4 bond distances in *n*Ace···RC also decrease by virtue of the introduction of the solvent molecule.

The solvent molecules not only impact the structures of *n*Ace···RC ($n = 1$−3) but also their complexation energies. The data in Table 2 indicate that although ΔE^{comp}_{RC} values become more negative in the microsolvation case than in the solvent-free case, ΔG^{comp}_{RC} values of *n*Ace···RC ($n = 1$−3) are still positive, suggesting that these complexes are unstable due to the substantial loss of entropy,[26] similar to the anionic and solvent−free ion pair S_N2 reactions in acetone.

3.2.2. TS Structures with Microsolvated Nucleophile and Barrier Heights. The TS geometries of microsolvated ion pair S_N2 reactions are significantly changed upon microsolvation of the nucleophile. As shown in Figures 3 and 4, due to the coordination of acetone on the positively charged Na atom, one acetone molecule, as a bridge, is located between Na and leaving X atom, leading to the absence of a direct interaction of Na and X atom, thus yielding the remarkable increase of O2···C5···X4 angle from about 125° in the solvent-free ion pair TS to 172° in the microsolvated ion pair TSs. The approximately linear conformations, similar to those of the anionic S_N2 TSs, will significantly release the strain in the solvent-free ion pair TS, leading to a lower barrier for the TSs with microsolvation of the ion pair nucleophile. Although there are geometrical similarities for microsolvated ion pair and anionic TSs, the nucleophilic site is closer to the central carbon, and the C−X distances become longer by about 0.1 Å due to the weaker nucleophilicity and steric effect from the microsolvated ion pair nucleophile. These TS geometrical changes result in the characteristics of the microsolvated ion pair TSs, but the anionic TSs are still tighter with shorter C5−O2 and C5−X4 distances than those in solvent-free ion pair TSs. It is also found that the distance between Na and nucleophilic oxygen becomes longer and longer with successive coordination of solvent molecules, thus increasing the interaction between $Na^{\delta+}$ and the carbonyl oxygen, accompanying the shortening of the C1−O2 bond.

It is obvious that the great changes of the ion pair S_N2 TS geometries with the microsolvation of the nucleophile will markedly lower their barrier heights. The relative free energies in Table 2 show that the PCM-ΔG^{b} values are reduced by about 83.7 kJ/mol in the case of monomicrosolvation. More solvent molecules coordinating on the ion pair nucleophile can further change the barriers, but to a much lower extent. The PCM-ΔG^{b} values are only decreased by 18.4 and 6.7 kJ/mol toward CH_3Cl and by 15.9 and 4.6 kJ/mol toward CH_3Br from mono- to di- to trisolvation. For the reaction toward CH_3I,

DOI: 10.1021/acs.jpca.5b01045
J. Phys. Chem. A 2015, 119, 3878−3886

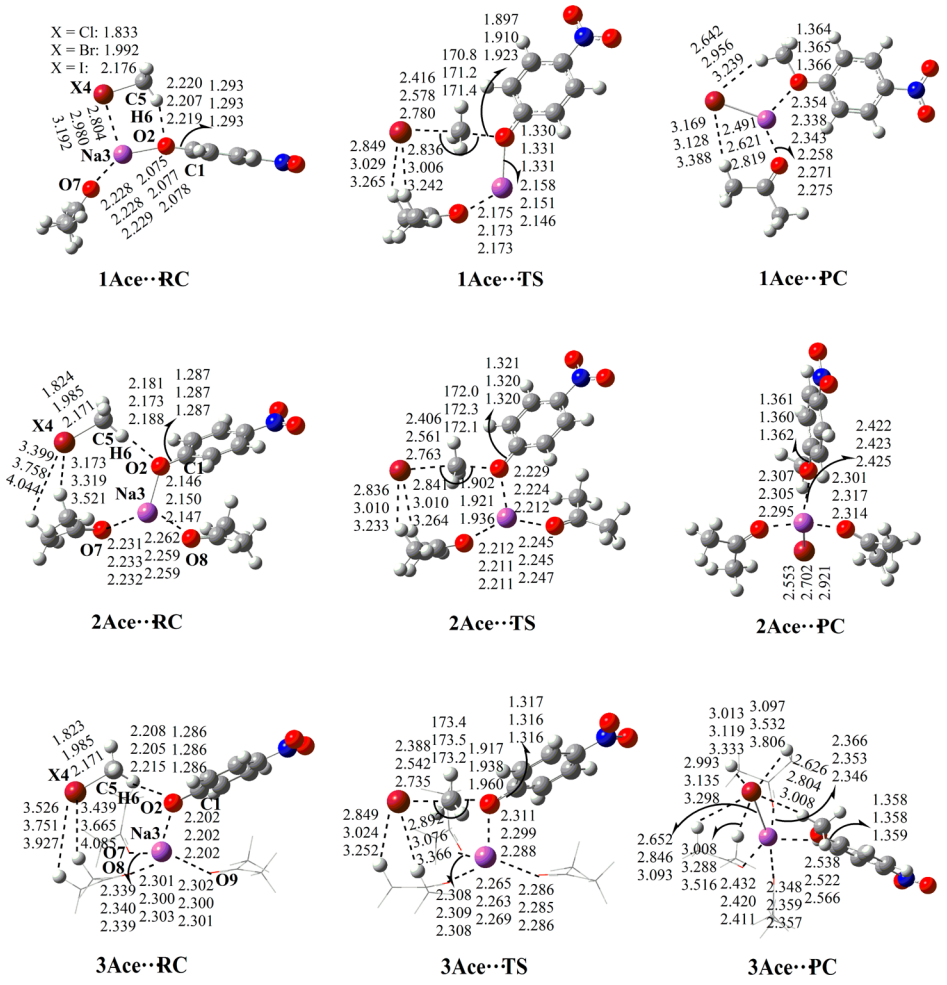

Figure 4. B3LYP/6-311+G(d,p)-optimized structures in the microsolvated ion pair S_N2 reactions *p*-NO_2−C_6H_4ONa···*n*Ace + CH_3X = *p*-NO_2−$C_6H_4OCH_3$ + *n*Ace···NaX (*n* = 1−3; X = Cl, Br, and I).

there is no further reduction of barrier with more solvent molecules coordinating on the ion pair nucleophile.

As shown in Table 2, the PCM-ΔG^b values for microsolvated ion pair S_N2 reactions are lower than those for the anionic ones by up to 18.4 kJ/mol (X = Cl, *n* = 3), 5.9 kJ/mol (X = Br, *n* = 3), and 6.7 kJ/mol (X = I, *n* = 1 and 2). These results clearly reveal that the most reactive nucleophile is the microsolvated ion pair, instead of the free anion and solvent-free ion pair. The highly strained solvent-free ion pair TS and higher solvation energy of free anion make it impossible for them to be active nucleophiles in acetone. The microsolvation of the ion pair plays a dominant role in enhancing the reactivity of the S_N2 reactions of sodium *p*-nitrophenoxide toward halomethanes in acetone, which is in agreement with the experimental observation.[24]

Careful inspection of the results in Table 2 also shows that two and three explicit acetone molecules involved in the microsolvation of the ion pair are favorable for the increase of the reaction rate of the title S_N2 reactions toward CH_3Cl and CH_3Br in acetone, whereas only monosolvation of the ion pair can enhance the reactivity of the title S_N2 reaction toward CH_3I, and almost no further effect is observed for additional explicit solvent molecules.

3.2.3. Importance of Bulk Solvent Effect on the Reactivity of Nucleophiles in Acetone. In order to show the bulk solvent effect on the reactivity of nucleophiles in acetone, we make a comparison of PCM-MP2/6-311+G(d,p)//B3LYP/6-311+G(d,p) (Table 2) and MP2/6-311+G(d,p)//B3LYP/6-311+G(d,p) results (Table S2 in the Supporting Information). Generally speaking, the absence of the continuum model will lower the overall barriers for both of the anionic and solvent-free ion pair S_N2 reactions and elevates the overall barriers of microsolvated ion pair S_N2 reactions due to the higher solvation energy of anionic and solvent-free ion pair species in the former cases. Moreover, the reactivity order in acetone, microsolvated ion pair > anion > solvent-free ion pair, is different from that in the gas phase, anion > microsolvated ion pair > solvent-free ion pair. This order indicates that the solvent-free ion pair is not the active nucleophile in all cases, and the barrier elevation of the anionic nucleophile in acetone by 16.7−25.1 kJ/mol can be attributed to its higher solvation energy. The continuum model lowering the barrier of the microsolvated ion pair may be explained by less solvation effects on the nucleophile, because most of them have been considered to be microsolvated, which is in agreement with the experiments. All of these results suggest the combined supramolecular/continuum model is very important in reasonably describing the reactivity of a nucleophile in polar solution.

3.3. Probing the Origin of Enhanced Reactivity for the Microsolvated Ion Pair Nucleophile by the Activation Strain Model. To shed further light on the origin of the enhanced reactivity for the title reaction in acetone, the

DOI: 10.1021/acs.jpca.5b01045
J. Phys. Chem. A 2015, 119, 3878−3886

activation strain model (ASM)[65−67] is applied to analyze the controlling factors of nucleophile reactivity. According to ASM, the overall free energy of activation (PCM-ΔG^b) is divided into the deformation energy (PCM-ΔG_{def}) and the interaction energy between the deformed reactants in the TS (PCM-ΔG_{int}). Due to the good correlations between PCM-ΔG^b and PCM-ΔE^b ($R^2 \approx 0.99$, Figure S1), it is acceptable to replace PCM-ΔG^b with PCM-ΔE^b in the ASM analysis.

The calculated PCM-ΔE_{def}, ΔE_{int}, and ΔE^b values for free anion and solvent-free and microsolvated ion pair are presented in Table 3 and Figure 5. The PCM-ΔE_{def} values decrease from

Table 3. PCM-MP2 Deformation Energies (ΔE_{def}) and Interaction Energies (ΔE_{int}) in the TSs and Overall Barriers (ΔE^b) (all in kJ/mol) without ZPVE Corrections for All the Reaction Paths in Acetone

X	paths	ΔE_{def}	ΔE_{int}	ΔE^b
Cl	Nu^-	167.8	−86.6	81.2
	0Ace···Nu	219.7	−33.5	186.2
	1Ace···Nu	203.3	−129.7	73.6
	2Ace···Nu	198.3	−132.6	65.7
	3Ace···Nu	198.7	−136.0	62.8
Br	Nu^-	134.3	−82.8	51.5
	0Ace···Nu	191.6	−28.9	162.8
	1Ace···Nu	177.4	−124.7	52.7
	2Ace···Nu	170.3	−124.7	45.6
	3Ace···Nu	172.0	−125.5	46.0
I	Nu^-	114.2	−62.3	51.9
	0Ace···Nu	179.1	−52.7	126.4
	1Ace···Nu	164.8	−133.1	31.8
	2Ace···Nu	158.6	−118.8	39.7
	3Ace···Nu	157.7	−113.8	43.9

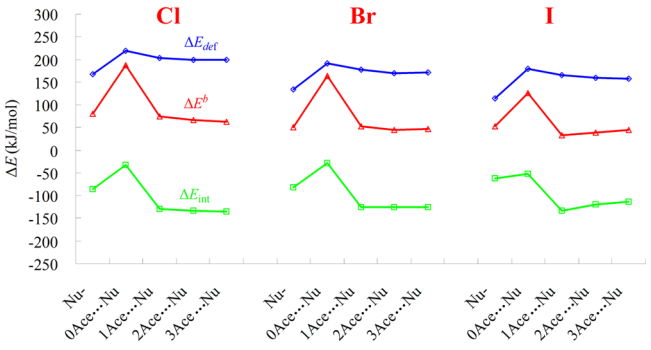

Figure 5. Variations of MP2 deformation electronic energies (PCM-ΔE_{def}) (in blue), interaction energies between the deformed reactants (PCM-ΔE_{int}) (in green), and overall barriers PCM-ΔE^b (in red) without ZPVE corrections for the different paths of the title reactions in acetone.

Cl to Br to I for all the reaction pathways, indicating the leaving ability I > Br > Cl. Moreover, the PCM-ΔE_{def} values for solvent-free ion pair TSs are larger than those in the other two cases due to their highly strained features. The smaller PCM-ΔE_{def} values are found in anionic and microsolvated TSs with similar linear geometries, in which the C−X distances in anionic TS are shorter than those in the latter cases, thus leading to the smallest deformation energies for anionic TSs. It is worth noting that the PCM-ΔE_{def} values are decreased only by about 12.6−16.7 kJ/mol from mono- to disolvated TS, whereas they vary in a smaller range from di- to trisolvated ion pair nucleophiles, because more solvent molecules only slightly change the TS geometries and most of the strain is released by the first acetone.

As shown in Table 3, the PCM-ΔE_{int} values become more negative from the solvent-free ion pair TSs (−28.9 to −52.7 kJ/mol) to the anionic TSs (−62.3 to −86.6) to the microsolvated ion pair TSs (−113.8 to −136.0 kJ/mol). The weaker interaction in the first case is obviously induced by the longer C5−O2 distance and the stronger repulsion between negatively charged O2 and leaving X atom. The stronger interactions in the anionic TSs may be from the free anionic nucleophile and the positively charged methyl cation. The more negative PCM-ΔE_{int} values are observed in the microsolvated ion pair TSs, indicating that the strongest interactions exist in *n*Ace···TS (n = 1−3), including the binding of solvent on Na atom, the electronic attraction between attacking oxygen and methyl cation, and the interaction between $X^{\delta-}$ and $H^{\delta+}$ atoms on acetone. Table 3 also shows that the PCM-ΔE_{int} values in the microsolvated cases vary in a small range of 6.3 kJ/mol for CH_3Cl, 3.8 kJ/mol for CH_3Br, and 19.2 kJ/mol for CH_3I, from mono- to trisolvation of nucleophile, indicating that the coordinating of the first acetone on the ion pair nucleophile is more important than that of the other two acetone molecules.

Generally, the larger PCM-ΔE_{def} value must be responsible for the higher barrier height, but the stronger interaction in the TS can lower the overall barrier. Figure 5 discloses that the relatively lower deformation energies and stronger interaction between the deformed reactants in the microsolvated TSs lead to lower barriers for the S_N2 reaction of microsolvated sodium *p*-nitrophenoxide toward halomethanes in acetone.

4. CONCLUDING REMARKS

Computational investigations on the kinetic performance for S_N2 reactions of sodium *p*-nitrophenoxide with halomethanes (CH_3X, X = Cl, Br, and I) in acetone solution were performed at the PCM-MP2/6-311+G(d,p)//B3LYP/6-311+G(d,p) level of theory. Our results indicate that the title S_N2 reaction may begin with the microsolvation of sodium *p*-nitrophenoxide, then the microsolvated ion pair acts as an active nucleophile to attack the central carbon, forming the key transition state structure, which exhibits a similar linear conformation as the anionic TS structure. In the microsolvated ion pair TS, one acetone is located between Na and X as a bridge. The explicit acetone molecules actually play a catalytic role in the S_N2 reaction of *p*-nitrophenoxide with halomethanes in pure acetone. The involvement of solvent molecule in the ion pair nucleophile not only significantly releases the high strain in the solvent-free ion pair TS, producing a smaller deformation energy, but also enhances the interaction between deformed reactants in the microsolvated ion pair TS with respect to solvent-free ion pair TS based on the activation strain analysis. Neither free *p*-nitrophenoxide anion nor solvent-free sodium *p*-nitrophenoxide is favored to be a reactive nucleophile in pure acetone.

It is worth noting that the order of nucleophilic reactivity, anion > solvent-free ion pair > microsolvated ion pair, from PCM-B3LYP/6-311+G(d,p) single-point calculations in acetone on the B3LYP/6-311+G(d,p)-optimized geometries in the gas phase (see Table S3 in the Supporting Information), cannot explain the experimental observation, indicating that the method adopted by us, i.e., single-point PCM-MP2 calculations

DOI: 10.1021/acs.jpca.5b01045
J. Phys. Chem. A 2015, 119, 3878−3886

in acetone on the B3LYP gas-phase geometries, is reliable for the present study. .

In summary, the present calculations reveal the mechanism of acetone-mediated S_N2 reaction by applying the supramolecular/continuum model and further demonstrate the important role of explicit solvent molecule in the study of the S_N2 reaction in the solution phase.

■ ASSOCIATED CONTENT

Supporting Information

Geometries and energies of all stationary points along the potential energy profile at the B3LYP/6-311+G(d,p) level of theory and relative energies at MP2/6-311+G(d,p)//B3LYP/6-311+G(d,p) and PCM-B3LYP/6-311+G(d,p)//B3LYP/6-311+G(d,p). This material is available free of charge via the Internet at http://pubs.acs.org.

■ AUTHOR INFORMATION

Corresponding Author

*E-mail: renyi@scu.edu.cn. Tel: +(86)-28-85412290.

Notes

The authors declare no competing financial interest.

■ ACKNOWLEDGMENTS

This project is supported by the Research Fund of Department of Education, Sichuan Province (Grant No. 13ZB0160). Y.R. also thanks the Open Research Fund of State Key Laboratory of Physical Chemistry of Solid Surfaces, Xiamen University (No. 201410), and the Open Research Fund of Key Laboratory of Advanced Scientific Computation, Xihua University (No. szjj2013-024).

■ REFERENCES

(1) Lowry, T. H.; Richardson, K. S. *Mechanism and Theory in Organic Chemistry*, 3rd ed.; Harper & Row: New York, 1987.

(2) Shaik, S. S.; Schlegel, H. B.; Wolfe, S. *Theoretical Aspects of Physical Organic Chemistry: The S_N2 Mechanism*; Wiley & Sons: New York, 1992.

(3) Williams, A. *Concerted and Bio-Organic Mechanisms*; CRC Press LLC: Boca Raton, FL, 2000.

(4) Laerdahl, J. K.; Uggerud, E. Gas Phase Nucleophilic Substitution. *Int. J. Mass. Spectrom.* **2002**, *214*, 277−3114 and references cited therein..

(5) Parker, A. J. Protic−Dipolar Aprotic Solvent Effects on Rates of Bimolecular Reactions. *Chem. Rev.* **1969**, *69*, 1−32 and references cited therein..

(6) Vayner, G.; Houk, K. N.; Jorgensen, W. L.; Brauman, J. I. Steric Retardation of S_N2 Reactions in the Gas Phase and Solution. *J. Am. Chem. Soc.* **2004**, *126*, 9054−9058.

(7) Hu, W. P.; Truhlar, D. G. Modeling Transition State Solvation at the Single-Molecule Level: Test of Correlated Ab Initio Predictions against Experiment for the Gas-Phase S_N2 Reaction of Microhydrated Fluoride with Methyl Chloride. *J. Am. Chem. Soc.* **1994**, *116*, 7797−7800.

(8) Alexander, R.; Ko, E. C. F.; Parker, A. J.; Broxton, T. J. Solvation of Ions. XIV. Protic−Dipolar Aprotic Solvent Effects on Rates of Bimolecular Reactions. Solvent Activity Coefficients of Reactants and Transition States at 25°. *J. Am. Chem. Soc.* **1968**, *90*, 5049−5069.

(9) Almerindo, G. I.; Pliego, J. R., Jr. Ab Initio Study of the S_N2 and E2 Mechanisms in the Reaction between the Cyanide Ion and Ethyl Chloride in Dimethyl Sulfoxide Solution. *Org. Lett.* **2005**, *7*, 1821−1823.

(10) Tondo, D. W.; Pliego, J. R., Jr. Modeling Protic to Dipolar Aprotic Solvent Rate Acceleration and Leaving Group Effects in S_N2 Reactions: A Theoretical Study of the Reaction of Acetate Ion with Ethyl Halides in Aqueous and Dimethyl Sulfoxide Solutions. *J. Phys. Chem. A* **2005**, *109*, 507−511.

(11) Pliego, J. R., Jr.; Piló-Veloso, D. Effects of Ion-Pairing and Hydration on the S_NAr Reaction of the F^- with *p*-chlorobenzonitrile in Aprotic Solvents. *Phys. Chem. Chem. Phys.* **2008**, *10*, 1118−1124.

(12) Streitwieser, A. Ion Pair Aggregates and Reactions; Experiment and Theory. *J. Mol. Model.* **2006**, *12*, 673−680.

(13) Suk, I.; Jang, S. W.; Kim, H. R.; Oh, Y. H.; Park, S. W.; Lee, S.; Chi, D. Y. A Mechanistic Study of S_N2 Reaction in a Diol Solvent. *J. Phys. Chem. A* **2009**, *113*, 3685−3689.

(14) Lee, S. S.; Kim, H. S.; Hwang, T. K.; Oh, Y. H.; Park, S. W.; Lee, S.; Lee, B. S.; Chi, D. Y. Efficiency of Bulky Protic Solvent for S_N2 Reaction. *Org. Lett.* **2008**, *10*, 61−64.

(15) Oh, Y. H.; Ahn, D. S.; Chung, S. Y.; Jeon, J. H.; Park, S. W.; Oh, S. J.; Kim, D. W.; Kil, H. S.; Chi, D. Y.; Lee, S. Facile S_N2 Reaction in Protic Solvent: Quantum Chemical Analysis. *J. Phys. Chem. A* **2007**, *111*, 10152−10161.

(16) Alunni, S.; Pero, A.; Reichenbach, G. Reactivity of Ions and Ion Pairs in the Nucleophilic Substitution Reaction on Methyl *p*-Nitrobenzenesulfonate. *J. Chem. Soc., Perkin Trans.* **1998**, *2*, 1747−1750.

(17) Winstein, S.; Savedoff, L. G.; Smith, S. G.; Stevens, I. D. R.; Gall, J. S. Ion Pairs, Nucleophilicity and Salt Effects in Bimolecular Nucleophilic Substitution. *Tetrahedron Lett.* **1960**, *1*, 24−30.

(18) Streitwieser, A.; Juaristi, E.; Kim, Y. J.; Pugh, J. Effect of Solvent on Aggregation and Reactivity of Two Lithium Enolates. *Org. Lett.* **2000**, *2*, 3739−3741.

(19) Kim, D. W.; Ahn, D. S.; Oh, Y. H.; Lee, S.; Kil, H. S.; Oh, S. J.; Lee, S. J.; Kim, J. S.; Ryu, J. S.; Moon, D. H.; Chi, D. Y. A New Class of S_N2 Reactions Catalyzed by Protic Solvents: Facile Fluorination for Isotopic Labeling of Diagnostic Molecules. *J. Am. Chem. Soc.* **2006**, *128*, 16394−16397.

(20) Fang, Y. R.; Westaway, K. C. Isotope Effects in Nucleophilic Substitution Reactions. VIII. The Effect of the Form of the Reacting Nucleophile on the Transition State Structure of an S_N2 Reaction. *Can. J. Chem.* **1991**, *69*, 1017−1021.

(21) Westaway, K. C.; Lai, Z. G. Solvent Effects on S_N2 Transition State Structure. II: The Effect of Ion Pairing on the Solvent Effect on Transition State Structure. *Can. J. Chem.* **1989**, *67*, 345−349.

(22) Westaway, K. C.; Lai, Z. G. Isotope Effects in Nucleophilic Substitution Reactions. VI. The Effect of Ion Pairing on the Transition State Structure of S_N2 Reactions. *Can. J. Chem.* **1988**, *66*, 1263−1271.

(23) Lai, Z. G.; Westaway, K. C. Isotope Effects in Nucleophilic Substitution Reactions. VII. The Effect of Ion Pairing on the Substituent Effects on S_N2 Transition State Structure. *Can. J. Chem.* **1989**, *67*, 21−26.

(24) Humeres, E.; Nunes, R. J.; Machado, V. G.; Gasques, M. D. G.; Machado, C. Ion−Dipole S_N2 Reaction in Acetone−Water Mixtures. Electrostatic and Specific Solute−Solvent Interactions. *J. Org. Chem.* **2001**, *66*, 1163−1170.

(25) Ooi, T.; Maruoka, K. Recent Advances in Asymmetric Phase-Transfer Catalysis. *Angew. Chem., Int. Ed.* **2007**, *46*, 4222−4266.

(26) Ando, K.; Morokuma, K. DFT and ONIOM Study on the Alkylation of the Lithium Enolate in Solution: Microsolvation Cluster Models for $CH_2{=}CHOLi + CH_3Cl + (THF)_{0-6}$. *Theor. Chem. Acc.* **2011**, *130*, 323−331.

(27) Gupta, L.; Ramírez, A.; Collum, D. B. Reaction of Lithium Diethylamide with an Alkyl Bromide and Alkyl Benzenesulfonate: Origins of Alkylation, Elimination, and Sulfonation. *J. Org. Chem.* **2010**, *75*, 8392−8399.

(28) Harder, S.; Streitwieser, A.; Petty, J. T.; Schleyer, P. V. R. Ion Pair S_N2 Reactions. Theoretical Study of Inversion and Retention Mechanisms. *J. Am. Chem. Soc.* **1995**, *117*, 3253−3259.

(29) Streitwieser, A.; Choy, G. S. C.; Abu-Hasanayn, F. Theoretical Study of Ion Pair S_N2 Reactions: Ethyl vs Methyl Reactivities and Extension to Higher Alkyls. *J. Am. Chem. Soc.* **1997**, *119*, 5013−5019.

(30) Leung, S. S. W.; Streitwieser, A. Theoretical Study of Structure of Alkali Metal Cyanates and Isocyanates and Their Related Ion Pair S_N2 Reactions. *J. Comput. Chem.* **1998**, *19*, 1325−1336.

DOI: 10.1021/acs.jpca.5b01045
J. Phys. Chem. A 2015, 119, 3878−3886

(31) Ren, Y.; Chu, S. Y. Modified Gaussian-2 Level Investigation of the Identity Ion-Pair S_N2 Reactions of Lithium Halide and Methyl Halide with Inversion and Retention Mechanisms. *J. Comput. Chem.* **2004**, *25*, 461−467.
(32) Ren, Y.; Chu, S. Y. Ion Pair S_N2 Reactions at Nitrogen: A High-Level G2M(+) Computational Study. *J. Phys. Chem. A* **2004**, *108*, 7079−7086.
(33) Ren, Y.; Gai, J. G.; Xiong, Y.; Lee, K. H.; Chu, S. Y. Theoretical Study on the Identity Ion Pair S_N2 Reactions of LiX with CH_3SX (X = Cl, Br, and I): Structure, Mechanism, and Potential Energy Surface. *J. Phys. Chem. A* **2007**, *111*, 6615−6621.
(34) Xiong, Y.; Ren, Y.; Chu, S. Y. A Theoretical Study of the Gas-Phase Ion Pair S_N2 Reactions of Lithium Halide and Methyl Halide with Inversion and Retention Mechanisms. *J. Mol. Struct. (THEOCHEM)*. **2003**, *664*−*665*, 279−289.
(35) Ren, Y.; Wang, X.; Chu, S. Y.; Wong, N. B. Counter-Ion Effect in the Nucleophilic Substitution Reactions at Silicon: A G2M(+) Level Theoretical Investigation. *Theor. Chem. Acc.* **2008**, *119*, 407−411.
(36) Ren, Y.; Chu, S. Y. Recent Development in the Study of S_N2 Reactions at Heteroatoms and Ion Pair Systems. *J. Theor. Comput. Chem.* **2006**, *5*, 1−20.
(37) Hasanayn, F.; Streitwieser, A.; Al-Rifai, R. A Computational Study of the Effect of Bending on Secondary Kinetic Isotope Effects in S_N2 Transition States. *J. Am. Chem. Soc.* **2005**, *127*, 2249−2255.
(38) Streitwieser, A.; Jayasree, E. G.; Leung, S. S. H.; Choy, G. S. C. A Theoretical Study of Substituent Effects on Allylic Ion and Ion Pair S_N2 Reactions. *J. Org. Chem.* **2005**, *70*, 8486−8491.
(39) Streitwieser, A.; Jayasree, E. G. Theoretical Study of the Effect of Coordinating Solvent on Ion Pair S_N2 Reactions: The Role of Unsymmetrical Transition Structures. *J. Org. Chem.* **2007**, *72*, 1785−1798.
(40) Streitwieser, A.; Jayasree, E. G.; Hasanayn, F.; Leung, S. S. H. A Theoretical Study of S_N2' Reactions of Allylic Halides: Role of Ion Pairs. *J. Org. Chem.* **2008**, *73*, 9426−9434.
(41) Tomasi, J.; Persico, M. Molecular Interactions in Solution: An Overview of Methods Based on Continuous Distributions of the Solvent. *Chem. Rev.* **1994**, *94*, 2027−2094.
(42) Becke, A. D. Density-Functional Thermochemistry. III. The Role of Exact Exchange. *J. Chem. Phys.* **1993**, *98*, 5648−5652.
(43) Lee, C.; Yang, W.; Parr, R. G. Development of the Colle−Salvetti Correlation−Energy Formula into a Functional of the Electron Density. *Phys. Rev. B* **1988**, *37*, 785−789.
(44) Miehlich, B.; Savin, A.; Stoll, H.; Preuss, H. Results Obtained with the Correlation Energy Density Functionals of Becke and Lee, Yang and Parr. *Chem. Phys. Lett.* **1989**, *157*, 200−206.
(45) Galabov, B.; Nikolova, V.; Wilke, J. J.; Schaefer, H. F., III; Allen, W. D. Origin of the S_N2 Benzylic Effect. *J. Am. Chem. Soc.* **2008**, *130*, 9887−9896.
(46) Westaway, K. C.; Fang, Y. R.; MacMillar, S.; Matsson, O.; Poirier, R. A.; Islam, S. M. A New Insight into Using Chlorine Leaving Group and Nucleophile Carbon Kinetic Isotope Effects To Determine Substituent Effects on the Structure of S_N2 Transition States. *J. Phys. Chem. A* **2007**, *111*, 8110−8120.
(47) Ruff, F.; Farkas, Ö.; Kucsman, Á. Computational Study of Reactivity and Transition Structures in Nucleophilic Substitutions on Benzyl Bromides. *Eur. J. Org. Chem.* **2006**, *24*, 5570−5580.
(48) Ruff, F.; Farkas, Ö. A DFT Study of Transition Structures and Reactivity in Solvolyses of *tert*-Butyl Chloride, Cumyl Chlorides, and Benzyl Chlorides. *J. Phys. Org. Chem.* **2008**, *21*, 53−61.
(49) Ochran, R. A.; Uggerud, E. S_N2 Reactions with Allylic Substrates—Trends in Reactivity. *Int. J. Mass Spectrom.* **2007**, *265*, 169−175.
(50) Fábiána, A.; Ruffa, F.; Farkas, Ö. Mechanism of Nucleophilic Substitutions at Phenacyl Bromides with Pyridines. A Computational Study of Intermediate and Transition State. *J. Phys. Org. Chem.* **2008**, *21*, 988−996.
(51) Ruff, F.; Farkas, Ö. Effect of Substituents on Activation Parameters in Aliphatic S_N2 Reactions. A DFT Study. *J. Org. Chem.* **2006**, *71*, 3409−3416.
(52) Li, Q. G.; Xue, Y. Effects of Substituent and Leaving Group on the Gas-Phase S_N2 Reactions of Phenoxides with Halomethanes: A DFT Investigation. *J. Phys. Chem. A* **2009**, *113*, 10359−10366.
(53) Wadt, W. R.; Hay, P. J. Ab Initio Effective Core Potentials for Molecular Calculations. Potentials for Main Group Elements Na to Bi. *J. Chem. Phys.* **1985**, *82*, 284−298.
(54) Frisch, M. J.; Trucks, G. W.; Schlegel, H. B.; Scuseria, G. E.; Robb, M. A.; Cheeseman, J. R.; Scalmani, G.; Barone, V.; Mennucci, B.; Petersson, G. A. et al. *Gaussian 09*, Revision A0; Gaussian, Inc., Wallingford CT, 2009.
(55) Bento, A. P.; Bickelhaupt, F. M. Nucleophilicity and Leaving-Group Ability in Frontside and Backside S_N2 Reactions. *J. Org. Chem.* **2008**, *73*, 7290−7299.
(56) Glukhovtsev, M. N.; Pross, A.; Schlegel, H. B.; Bach, R. D.; Radom, L. Gas-Phase Identity S_N2 Reactions of Halide Anions and Methyl Halides with Retention of Configuration. *J. Am. Chem. Soc.* **1996**, *118*, 11258−11264.
(57) Glukhovtsev, M. N.; Pross, A.; Radom, L. Gas-Phase Identity S_N2 Reactions of Halide Anions with Methyl Halides: A High-Level Computational Study. *J. Am. Chem. Soc.* **1995**, *117*, 2024−2032.
(58) *NIST Computational Chemistry Comparison and Benchmark Database. NIST Standard Reference Database Number 101, Release 16a, August 2013*; Johnson III, R. D., Ed.; http://cccbdb.nist.gov/.
(59) Jensen, T.; Brodersen, S.; Guelachvili, G. Determination of A_0 for $CH_3{}^{35}Cl$ and $CH_3{}^{37}Cl$ from the ν_4 Infrared and Raman Bands. *J. Mol. Spectrosc.* **1981**, *88*, 378−393.
(60) Graner, G. The Methyl Bromide Molecule: A Critical Consideration of Perturbations in Spectra. *J. Mol. Spectrosc.* **1981**, *90*, 394−438.
(61) Hannonv, M. D.; Laurie, V. W.; Kuczkowski, R. L.; Ramsav, D. A.; Lovas, F. J.; Lafferty, W. J.; Maki, A. G. Molecular Structures of Gas-Phase Polyatomic Molecules Determined by Spectroscopic Methods. *J. Phys. Chem. Ref. Data.* **1979**, *8*, 619−721.
(62) *CRC Handbook of Chemistry and Physics*, 72th ed.; Lide, D. R., Ed.; CRC Press: Boca Raton, FL, 1991.
(63) *CRC Handbook of Chemistry and Physics*, 86th ed.; Lide, D. R., Ed.; CRC Press: Boca Raton, FL, 2005.
(64) Rao, J. S.; Dinadayalane, T. C.; Leszczynski, J.; Sastry, G. N. Comprehensive Study on the Solvation of Mono- and Divalent Metal Cations: Li^+, Na^+, K^+, Be^{2+}, Mg^{2+} and Ca^{2+}. *J. Phys. Chem. A* **2008**, *112*, 12944−12953.
(65) Bickelhaupt, F. M. Understanding Reactivity with Kohn−Sham Molecular Orbital Theory: E2−S_N2 Mechanistic Spectrum and Other Concepts. *J. Comput. Chem.* **1999**, *20*, 114−128.
(66) van Zeist, W.-J.; Bickelhaupt, F. M. The Activation Strain Model of Chemical Reactivity. *Org. Biomol. Chem.* **2010**, *8*, 3118−3127.
(67) Ren, Y.; Wei, X. G.; Ren, S. J.; Lau, K. C.; Wong, N. B.; Li, W. K. The α-Effect Exhibited in Gas-Phase S_N2@N and S_N2@C Reactions. *J. Comput. Chem.* **2013**, *34*, 1997−2005.

DOI: 10.1021/acs.jpca.5b01045
J. Phys. Chem. A 2015, 119, 3878−3886